

Complexity growth of operators in the SYK model and in JT gravity

Shao-Kai Jian,¹ Brian Swingle,² and Zhuo-Yu Xian³

¹*Condensed Matter Theory Center, Department of Physics,
University of Maryland, College Park, Maryland 20742, USA**

²*Department of Physics, Brandeis University, Waltham,
Massachusetts 02453, USA and Condensed Matter Theory Center,
Department of Physics, University of Maryland,
College Park, Maryland 20742, USA[†]*

³*CAS Key Laboratory of Theoretical Physics, Institute of Theoretical Physics,
Chinese Academy of Sciences, Beijing, 100190, China[‡]*

Abstract

The concepts of operator size and computational complexity play important roles in the study of quantum chaos and holographic duality because they help characterize the structure of time-evolving Heisenberg operators. It is particularly important to understand how these microscopically defined measures of complexity are related to notions of complexity defined in terms of a dual holographic geometry, such as complexity-volume (CV) duality. Here we study partially entangled thermal states in the Sachdev-Ye-Kitaev (SYK) model and their dual description in terms of operators inserted in the interior of a black hole in Jackiw-Teitelboim (JT) gravity. We compare a microscopic definition of complexity in the SYK model known as K-complexity to calculations using CV duality in JT gravity and find that both quantities show an exponential-to-linear growth behavior. We also calculate the growth of operator size under time evolution and find connections between size and complexity. While the notion of operator size saturates at the scrambling time, our study suggests that complexity, which is well defined in both quantum systems and gravity theories, can serve as a useful measure of operator evolution at both early and late times.

* skjian@umd.edu

† bswingle@umd.edu

‡ xianzy@itp.ac.cn

CONTENTS

I. Introduction	2
II. K-complexity in the SYK model	7
A. Review of K-complexity	7
B. Dynamics of K-complexity in chaotic systems	8
C. K-complexity growth of operators in the SYK model	11
III. Holographic complexity in the JT gravity	13
A. Partially entangled thermal state in JT gravity	13
B. Holographic complexity growth of the Heisenberg operator	16
IV. The size of the partially entangled thermal state	19
A. The size from the SYK model	19
B. The size derived from JT gravity	20
C. Relation between the operator size and the complexity	21
V. Conclusion and outlook	21
Acknowledgement	22
A. K-complexity in the SYK model at early times	22
B. Summary of coordinate systems	23
C. Generating function for size at generic θ	23
D. About the scrambling time	24
References	24

I. INTRODUCTION

Depending on the timescales of interest, several interrelated concepts have recently been proposed to characterize the presence or absence of chaos in quantum dynamics. The basic expectation in a quantum chaotic system is that states in the Schrödinger picture and operators in the Heisenberg picture become more elaborate as time passes. For the purposes of this work, we wish to compare and contrast two ways to quantify this growth: the notion of size and the notion of complexity. We define these notions in detail below, but in brief, size is a measure of how many degrees of freedom are involved in a state or acted on by an operator while complexity refers to the number of elementary steps of some type needed to prepare a state or implement an operator. These two concepts are certainly interrelated in various ways, for example, a certain minimal complexity is required in order for an operator to have large size. In this work, we study and compare precise versions of these notions in two models: the Sachdev-Ye-Kitaev (SYK) model and 2d Jackiw-Teitelboim (JT) gravity.

It is useful to consider two regimes of time, corresponding to times before or after the system has come to approximate global equilibrium. The crossover time between these two regimes, called the scrambling time, will be defined in detail below. Roughly speaking, it refers to the time after which a small perturbation to the system has spread over the entire system.

Prior to the scrambling time, out-of-time order correlation functions (OTOCs) [1, 2] characterize the chaotic growth of Heisenberg operators of the form

$$O_\beta(\varphi) \equiv e^{-(1-2\varphi/\pi)\beta H/4} O e^{-(1+2\varphi/\pi)\beta H/4}, \quad \varphi = \theta + iu, \quad (1)$$

where H is the Hamiltonian, β is the inverse temperature, θ labels the location of the insertion in the imaginary-time evolution, and $u = 2\pi t/\beta$ is the real time in the unit of $\beta/2\pi$. For a simple operator O which disturbs only a few degrees of freedom, time evolution causes information about this disturbance to spread over the system whenever O is not conserved, $[H, O] \neq 0$, a process known as information scrambling [3–6]. For all-to-all chaotic Hamiltonians, information initially spreads exponentially fast with an exponent called a quantum Lyapunov exponent, until it scrambles over the whole system [1], as illustrated in Fig. 1. The number of degrees of freedom affected during this scrambling process is measured by the size n of the Heisenberg operator $O_\beta(\varphi)$ [7–10].

It will be convenient to translate the language of operators into the language of states using a standard operator-state mapping. The space of operators acting on a Hilbert space \mathcal{H} can be mapped to a state in two copies of the Hilbert space $\mathcal{H} \otimes \mathcal{H}$ by $O \rightarrow |O\rangle = O \otimes \mathbb{1} |0\rangle$ where $|0\rangle$ is a maximally entangled state in the doubled Hilbert space. It is convenient to fix a Hamiltonian H for one copy of the system and take $|0\rangle = \sum_n |E_n\rangle \otimes |E_n\rangle$ where $\{|E_n\rangle\}$ is a basis of energy eigenstates of H . This mapping is appropriate at infinite temperature; it can be extended to finite temperature using the (unnormalized) thermofield double (TFD) state $|\mathbb{1}_\beta\rangle = \sum_n e^{-\beta E_n/2} |E_n\rangle \otimes |E_n\rangle$ where $\mathbb{1}_\beta = e^{-\beta H/2}$ corresponds to $O = \mathbb{1}$ in (1). A general operator of the form (1) is mapped to a so-called partially entangled thermal state (PETS) $|O_\beta(\theta + iu)\rangle$ [11]. The evolution of the operator $O_\beta(\varphi) = U(t)^\dagger O_\beta(\theta) U(t)$ is mapped to the evolution of the state $|O_\beta(\varphi)\rangle \equiv U(-t) \otimes U(t) |O_\beta(\theta)\rangle$, where $U(t) = e^{-iHt}$ and the two copies evolve in opposite directions in time, e.g. with Hamiltonians H and $-H$. Without the insertion of O , the state $U(-t) \otimes U(t) |\mathbb{1}_\beta\rangle = |\mathbb{1}_\beta\rangle$ is invariant under time evolution. With the insertion of non-conserved O , the state is no longer invariant and the dynamics can be conveniently diagnosed using correlations between the two copies.

In the context of the SYK model made from N fermions ψ^i obeying $\{\psi^i, \psi^j\} = \delta^{ij}$ with q -body interactions, the operator growth structure is well understood in the large- q limit [7, 8] and the conformal limit [12]. Here the notion of size n of an operator is the number of elementary operators—the single Majorana operators ψ^j —contained in that operator. The growth of size can be detected by the decay of correlations between the two systems in the PETS state, which is equivalent to a kind of OTOC. More precisely, the size is $n[O_\beta(\varphi)] = N/2 - i \sum_j \langle O_\beta(\varphi) | \psi^j \otimes \psi^j | O_\beta(\varphi) \rangle / Z$, where the maximally entangled state $|0\rangle$ is defined by $(\psi^j \otimes \mathbb{1} - i\mathbb{1} \otimes \psi^j) |0\rangle = 0$, $\forall j = 1, \dots, N$ and the normalization factor is $Z = \langle O_\beta(\varphi) | O_\beta(\varphi) \rangle$.

The notion of size growth has also been explored in the context of holography. There the TFD state $|\mathbb{1}_\beta\rangle$ is dual to an eternal black hole in AdS space [13]. For $\theta = \pm\pi/2$, acting a simple operator O on the TFD state $|\mathbb{1}_\beta\rangle$ corresponds to releasing a particle on the asymptotic boundary. The gravity of the black hole forces the particle to fall into the interior of the bulk and affect the near horizon region, which is the holographic bulk counterpart of the boundary growth of size [14]. Operator size has also been conjectured to be dual to the momentum of the particle [12, 14–18]. It is therefore interesting to compare the SYK model and JT gravity model, which are closely related in the conformal limit of low temperatures [19, 20]. In particular, the size-momentum relation can be studied using $SL(2)$ generators that function as both generators of spacetime transformations and measures of size [12, 16].

Now consider the situation after the scrambling time. At these longer times, the operator size has reached its equilibrium value, but operators (and states) are still evolving unitarily in the massive many-body Hilbert space. In particular, the complexity of a Heisenberg operator, a quantity borrowed from quantum information theory, is conjectured to continue to grow with time long after the scrambling time [21, 22]. We illustrate the evolution after scrambling using

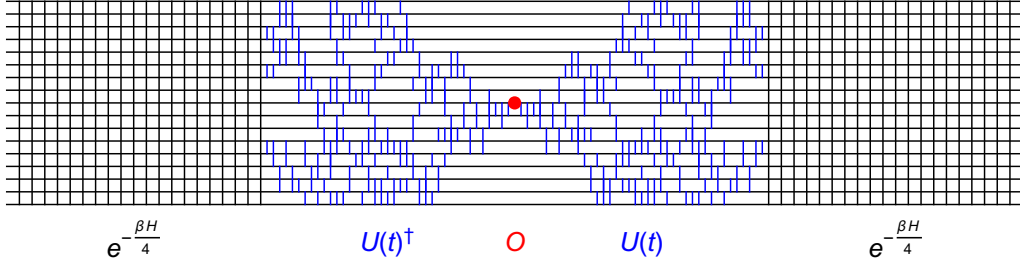


FIG. 1. A cartoon of a Heisenberg operator inserted at the half of the thermal circle. Some gates of $U(t)^\dagger$ and $U(t)$ on the unaffected channels have been canceled with each other, due to the switchback effect.

a schematic circuit diagram in Fig. 1. The most common type of complexity considered in this context is that of circuit complexity, which is defined as the minimal number of elementary quantum gates that are required to produce a target state or operator from a reference. In a chaotic system, it is believed that the circuit complexity of an initial state will grow linearly with time until a time of order the exponential of the system entropy [21–25].

Various definitions of complexity for unitary operators in quantum mechanics and quantum field theories have been proposed [6, 26, 27]. In this paper, we consider a different notion of complexity for hermitian operators, the K-complexity [28, 29], defined through a Krylov basis that is uniquely determined by the evolution Hamiltonian and the reference operator in question. Using the state-operator mapping, we can define this complexity in terms of states or operators; here we focus on PETS as the reference state. The Krylov basis is obtained as follows. In the operator language, one repeatedly applies the Liouvillian map $[H, \cdot]$ to an operator $O_\beta(\theta)$ to generate a basis of operators. In dual state representation, one generates a sequence of new states starting from a PETS, e.g. $[[H, O_\beta(\theta)]] = (H \otimes \mathbb{1} - \mathbb{1} \otimes H) |O_\beta(\theta)\rangle$. Note that, in the state language, the evolution generated by $H \otimes \mathbb{1} - \mathbb{1} \otimes H$ is called boost evolution due to the interpretation of this transformation as a boost in AdS/CFT. It is one of the $SL(2)$ generators mentioned above. Given this sequence of states (or operators), one then orthonormalizes them to produce the desired Krylov basis,

$$|O_{\beta,j}(\theta)\rangle \propto (H \otimes \mathbb{1} - \mathbb{1} \otimes H)^j |O_\beta(\theta)\rangle + \dots, \quad (2)$$

where j denotes the number of applications of the Liouvillian [30], and \dots comes from the Gram-Schmidt orthonormalization process. The target state can then be decomposed into the Krylov basis $|\Psi_T(t)\rangle = \sum_j i^j \phi_j(t) |O_{\beta,j}(\theta)\rangle$, where ϕ_j denotes the amplitude at j -th basis and the factor of i^j is for convenience. The K-complexity \mathcal{C}_K is then defined by declaring that basis element j has complexity j ,

$$\mathcal{C}_K |O_{\beta,j}(\theta)\rangle = j |O_{\beta,j}(\theta)\rangle, \quad (3)$$

so the average K-complexity of the target state $|\Psi_T(t)\rangle$ is

$$\mathcal{C}_K[|\Psi_T(t)\rangle] = \langle \Psi_T(t) | \mathcal{C}_K | \Psi_T(t) \rangle = \sum_j j |\phi_j(t)|^2. \quad (4)$$

K-complexity is somewhat analogous to a circuit complexity definition in which the elementary operation is not a unitary but a Hermitian generator of unitary evolution, the Liouvillian or boost generator $H \otimes \mathbb{1} - \mathbb{1} \otimes H$. The complexity can then be defined as an operator by fixing its eigenvectors and eigenvalues in terms of (3). Then one has a notion of average complexity by expanding general states in the Krylov basis (4). We will give more details of the definition K-complexity in the SYK model in the next section.

It was shown in [28] that the K-complexity grows exponentially with time before the scrambling time for a variety of chaotic Hamiltonians. At these early times, each application of the Liouvillian will increase the operator size by at most a constant amount. As a result, the Krylov basis has a close relation with the operator size at early times. Indeed, it turns out that the K-complexity bounds any properly defined notion of operator size [28]. After the scrambling time, the authors of [29] conjectured that the K-complexity of a chaotic system will continue to grow, now linearly with time, until it reaches a value that is exponential in the system size. The argument in [29] is based on the eigenstate thermalization hypothesis (ETH) applied to the chaotic Hamiltonian of interest [31–33]. Here we explicitly show that the late-time growth of the K-complexity is bounded by a linear function. We also numerically evaluate the K-complexity growth in the SYK model and indeed find linear growth after the scrambling time. Combined with previous results, our results demonstrate that K-complexity shows an exponential-to-linear growth pattern in the SYK model. We conjecture that this holds true for all chaotic systems, namely that after a short “dissipation time” typically set by the local energy scales of the problem, K-complexity shows a universal exponential growth dictated by a Lyapunov exponent which then gives way to linear growth after the scrambling time. Although we do not see a saturation of the K-complexity at late time due to the limited working precision in the calculation, it is expected that the linear growth of the K-complexity will finally saturate at a time that is exponential in the system size [29].

To complete the background for our story, we consider the role of complexity in holography. In that context, circuit complexity has received enormous recent attentions for its potential relation to various features of the dual holographic geometry, especially wormholes inside black holes [34]. Two conjectures on the duality of the complexity of a state were proposed. The complexity-volume (CV) conjecture states that the complexity is proportional to the volume of the maximal spatial surface (meaning spacetime codimension-one manifold) connecting the boundary of the dual eternal black hole [21]. The complexity-action (CA) conjecture states that the complexity is proportional to the action of the Wheeler-DeWitt patch [35, 36]. The proposal of holographic complexity inspires new understanding on the complexity in field theories [37–39] and in gravity [40–48].

In models with partial holographic duals, such as the SYK model, it is interesting to compare microscopic notions of complexity to holographic proposals. For the situation of interest to us, namely PETS states in the SYK model, we consider eternal black holes in JT gravity with a matter field which is dual to the operator O defining the PETS [11]. In this model of gravity, the problem of gravitational backreaction of the matter field can be mapped to the motion of particles in a hyperbolic space [11, 49]. Focusing on the CV duality for simplicity [21, 41], the holographic complexity becomes proportional to the geodesic distance between the two boundaries of the eternal black hole in JT gravity. Interestingly, this holographic complexity also exhibits an exponential-to-linear growth behavior for PETS. Similar behaviors of the complexity appear in the shock wave geometry, which caused by the matter falling into the black hole [17, 18].

Because of the similarities the microscopic K-complexity of SYK and the “course grained” complexity defined through the CV conjecture, it is very interesting to compare these two notions of complexity in detail. At early times, both complexities exhibit an exponential growth at a rate set by a quantum Lyapunov exponent. In JT gravity, what appears is the maximal Lyapunov exponent $2\pi/\beta$, with β is the inverse temperature. In the SYK model, one finds a temperature dependent Lyapunov exponent in the large- q approximation, and in the conformal limit, this exponent approaches the same $2\pi/\beta$ exponent as in gravity. We find that the K-complexity actually precisely matches the holographic complexity up to an unimportant constant before the scrambling time. Similarly, both complexities grow linearly after the scrambling time but with different slopes. The slope in the SYK model is set by microscopic scale while the slope in JT gravity is set by the temperature. Nevertheless, both are extensive in the system size and if we consider the rate of

complexity growth ratio, i.e.,

$$R(t) = \frac{d \log C(t)}{dt}, \quad (5)$$

where C refers to the complexity, then the two notions of complexity turn out to have the same rate up to times that are exponential in system entropy.

To summarize, both size and complexity provide useful windows into quantum chaotic dynamics depending on the timescale of interest. Still, it would be convenient if there a single quantity that could capture the relevant physics of both quantities. This is not a implausible request since as the size of an operator grows, the complexity is increasing. Indeed, it has been proposed that the growth of operator size is proportional to the rate of increase of its complexity [50]. Actually, three seemingly distinct quantities in holography—operator size, complexity, and radial momentum—are proposed to be closely related to each other [15, 17, 18, 51], as schematically shown by the following equation,

$$\frac{n}{\bar{\beta}} \sim P \sim \frac{dC(t)}{dt}, \quad (6)$$

where $1/\bar{\beta}$ represents an energy scale that sets units, and n and P refer to the operator size and the momentum, respectively. To verify this relation, we also carry out a calculation of operator size of the PETS in the SYK model and the corresponding $SL(2)$ charge in JT gravity. The results show agreement with both K-complexity and holographic complexity up to the scrambling time. In this sense, the complexity serves as a useful quantity that can capture the dynamics of a simple Heisenberg operator in chaotic systems at both early and late times. While we focused on chaotic systems here, it would be interesting to explore the notion of complexity in integrable systems as well [28].

The rest of this paper is organized as follows. In Sec. II, we explore the dynamics of the K-complexity in the SYK model. We first review the definition of K-complexity, in which the Lanczos coefficient plays an important role. The dynamics of the K-complexity is mapped to a particle moving in one-dimensional lattice made up of the Krylov basis. Then a proof concerning the late-time linear growth of K-complexity is given using a bound on the Lanczos coefficients. We also evaluate the K-complexity in the SYK model, and show that it exhibits exponential-to-linear growth. In Sec. III, we calculate the holographic complexity of the PETS in JT gravity. The insertion of a simple operator causes a perturbation to the TFD state, which can mapped to an insertion of a particle moving in the hyperbolic space. The backreaction from the operator insertion can be easily captured at the Schwarzian limit. Then the holographic complexity is measured by the geodesic connecting two asymptotic boundaries of the AdS_2 spacetime. The dynamics of the microscopic K-complexity and the holographic complexity share many similarities, and in certain aspect the K-complexity is a microscopic candidate of the holographic complexity. In Sec. IV, the relation between the operator size and the complexity growth rate is considered. We calculate the size of the PETS in both the SYK model and JT gravity. In particular the size is linearly related to the $SL(2)$ charges of AdS_2 spacetime. We also verify that the growth rate of both K-complexity and holographic complexity of the PETS is given by its size in the Lyapunov regime. As a result, the notion of complexity is able to characterize the dynamics of Heisenberg operators in chaotic systems at both short and long time scales. In Appendix A, we review the finite temperature generalization of K-complexity. In Appendix B, we summarize various coordinate systems of AdS_2 . In Appendix C, we obtain the generating function of size operator at generic inserting angle. In Appendix D, we discuss the scrambling time of OTOC from the Schwarzian dynamics.

II. K-COMPLEXITY IN THE SYK MODEL

A. Review of K-complexity

This section reviews K-complexity associated with the Krylov basis in the SYK model. Unlike an a priori basis, the Krylov basis is uniquely determined by the evolution Hamiltonian and the initial state. As a result, the K-complexity is a natural notion capturing the intrinsic dynamics of the evolution operator, without the ambiguity of choosing an operator basis or elementary gates. We take the inner product in operator space A to be defined by the inner product in $\mathcal{H} \otimes \mathcal{H}$, namely $\langle O|O' \rangle = \text{Tr}[O^\dagger O']$, so the norm is $\|O\| = \langle O|O \rangle^{1/2}$.

We will work at infinite temperature in this section, which means the PETS is $|O_{\beta=0}(\theta)\rangle$, where θ is now irrelevant since the thermal circle is a point with no size. Hence, for notational simplicity, we neglect the subscript β and the angle variable θ , and denote the time evolved PETS by $|O_{\beta=0}(\varphi)\rangle = |O(t)\rangle$. It is convenient to normalize this operator such that $\|O\| = 1$. The Heisenberg evolution of an operator is generated by the Liouvillian $\mathcal{L} = [H, \cdot]$, *i.e.*, $|O(t)\rangle = e^{it\mathcal{L}} |O\rangle$. The Krylov basis is defined through the Liouvillian superoperator:

$$|O_0\rangle = |O\rangle, \quad b_0 = 0, \quad (7)$$

$$|O_n\rangle = b_n^{-1} |A_n\rangle, \quad |A_n\rangle = \mathcal{L} |O_{n-1}\rangle - b_{n-1} |O_{n-2}\rangle, \quad b_n = \|A_n\|, \quad n \geq 1. \quad (8)$$

The second line is merely carrying out a Gram-Schmidt procedure on the states $|A_n\rangle$ to produce the states $|O_n\rangle$. The iteration stops once the Liouvillian fails to generate a linearly independent state. The set of states generated typically span a space of dimension K that is of order $K \sim \dim \mathcal{H}^2$, but they do not always form a complete basis, $K \leq \dim \mathcal{H}^2$. In particular, this happens when the Hamiltonian has conserved charges. For example, the SYK Hamiltonian preserves fermion parity, so the Krylov basis spans the even (odd) fermion parity subspace if one starts with an even (odd) parity reference state.

In terms of the Krylov basis, the Liouvillian superoperator operator is a simple tridiagonal matrix,

$$L_{mn} = \langle O_m | \mathcal{L} | O_n \rangle = \delta_{n,m-1} b_{n+1} + \delta_{n,m+1} b_n. \quad (9)$$

The coefficients b_n are also known as Lanczos coefficients.

The Heisenberg operator corresponding to Hermitian O can be decomposed in Krylov basis, $|O(t)\rangle = \sum_{n=0}^m i^n \phi_n(t) |O_n\rangle$, with ϕ_n real. Unitary evolution implies $\sum_{n=0}^K |\phi_n|^2 = 1$, so ϕ_n can be understood as a wavefunction for the Heisenberg operator in the Krylov basis. The effective Schrödinger equation obeyed by the wavefunction is

$$\partial_t \phi_n(t) = b_n \phi_{n-1}(t) - b_{n+1} \phi_{n+1}(t), \quad \phi_0(0) = 1. \quad (10)$$

This Schrödinger equation (10) effectively describes a quantum particle moving in one dimensional chain in which each lattice site corresponds to an element of the Krylov basis. We note that this mapping from operators to quantum particles shares similar ideas with the mapping from unitary operators to points in a complexity geometry [22, 52].

Now, the K-complexity is defined as a linear operator \mathcal{C}_K which is diagonal in the Krylov basis and which simply counts the basis elements [28],

$$\mathcal{C}_K |O_n\rangle = n |O_n\rangle. \quad (11)$$

Thus, the average K-complexity of the Heisenberg operator $O(t)$ is the average position of the particle moving in the chain, *i.e.*,

$$C_K[O(t)] = \langle O(t) | \mathcal{C}_K | O(t) \rangle = \sum_{n=0}^K n |\phi_n(t)|^2. \quad (12)$$

The dynamics of K-complexity is governed by Lanczos coefficient through the Schrödinger equation (10). Following Ref. [29], we can build intuition by considering a continuum limit of the Schrödinger equation obtained by introducing a short-range cutoff ϵ with $x = \epsilon n$. Expanding (10) and keeping the lowest-order term in ϵ , we get a continuous version of the Schrödinger equation,

$$\partial_t \phi(x, t) = -v(x) \partial_x \phi(x, t) - \frac{1}{2} v'(x) \phi(x, t), \quad (13)$$

where the position-dependent velocity $v(x) = 2\epsilon b_n$ captures the information from the Lanczos coefficients. Using a coordinate transformation defined by $dy = \frac{dx}{v(x)}$, the wavefunction changes to $\psi(y, t) = \sqrt{v(x)} \phi(x, t)$, and the Schrödinger equation becomes a solvable wave equation,

$$(\partial_t + \partial_y) \psi(y, t) = 0, \quad \psi(y, t) = \psi_i(y - t), \quad (14)$$

where $\psi_i(y)$ is the initial wavefunction at $t = 0$. Note that ψ can also be understood as a wavefunction with normalization $1 = \frac{1}{\epsilon} \int dy |\psi(y, t)|^2$.

The average K-complexity of ψ is then

$$C_K(t) = \sum_n n |\phi_n(t)|^2 = \frac{1}{\epsilon^2} \int dx x |\phi(x, t)|^2 = \frac{1}{\epsilon^2} \int dy x v(x) |\phi(x, t)|^2 = \frac{1}{\epsilon^2} \int dy x(y) |\psi(y, t)|^2, \quad (15)$$

where, again, $x(y)$ is determined by the coordinator transformation $dy = \frac{dx}{v(x)}$.

Given a localized initial condition corresponding to the reference state, $|\psi_i(y)|^2 = \epsilon \delta(y)$, the average K-complexity is

$$C_K(t) = \frac{1}{\epsilon} \int dy x(y) \delta(y - t) = \frac{x(t)}{\epsilon}, \quad (16)$$

which is fully determined by $x(y)$ or, equivalently, by the velocity through $\frac{dx}{v(x)} = dy$.

For Lanczos coefficients given by $b_n = \alpha n^\delta$, the velocity is $v(x) = 2\alpha \epsilon (x/\epsilon)^\delta$. Hence, the K-complexity grows as

$$C_K(t) \sim \begin{cases} e^{2\alpha t}, & \delta = 1 \\ (2\alpha t)^{1/(1-\delta)}, & \delta < 1 \end{cases}. \quad (17)$$

In particular, for $\delta = 1$, the average K-complexity grows exponentially, while for $\delta = 0$, it grows linearly. Ref. [28] showed that the Lanczos coefficients are bounded by a linear function $n \ll N$, where N is the system size, implying that the average K-complexity grows at most exponentially up to the scrambling time, $\alpha t \sim \log N$. In the next section, we show that the Lanczos coefficients are bounded by a constant when $n \gg N$, and consequently, that the average K-complexity can grow no faster than linearly with time at late time.

B. Dynamics of K-complexity in chaotic systems

To bound the Lanczos coefficients, it is useful to consider moments of Liouvillian superoperator,

$$\mu_{2n} \equiv \langle O_0 | \mathcal{L}^{2n} | O_0 \rangle, \quad (18)$$

which are closely related to the OO Green function or auto-correlation function,

$$G(t) = \frac{\text{Tr}[O^\dagger(0)O(t)]}{\text{Tr}[O^\dagger O]} = \langle O_0 | e^{it\mathcal{L}} | O_0 \rangle = \sum_n \frac{(it)^{2n}}{(2n)!} \langle O_0 | \mathcal{L}^{2n} | O_0 \rangle = \sum_n \frac{(it)^{2n}}{(2n)!} \mu_{2n}, \quad (19)$$

$$\mu_{2n} = \int \frac{d\omega}{2\pi} \omega^{2n} G(\omega), \quad G(\omega) = \int dt e^{i\omega t} G(t). \quad (20)$$

Note that the Greens function is normalized such that $G(t = 0) = 1$.

Knowing the moments, one can get the Lanczos coefficients using an explicit relation between the two (e.g., see Appendix A of [28]). Here we need only the following bound,

$$\prod_{k=1}^n b_k^2 \leq \mu_{2n} \leq C_n \max_{\{b_k\}} (b_k^{2n}), \quad (21)$$

where $C_n = \frac{(2n)!}{n!(n+1)!}$ is the Catalan number. If the Lanczos coefficients have the asymptotic form $b_n = \alpha n^\delta$, as $n \rightarrow \infty$, then the moments have the asymptotic behavior

$$\mu_{2n} \approx (2\alpha)^{2n} e^{2\delta n \log n + o[n]}, \quad n \gg 1. \quad (22)$$

Now we show that the Lanczos coefficients are bounded by a constant for $n \gg N$. Take the Hilbert space to consist of N Majoranas (with N an even integer) and consider an all-to-all q -body Hamiltonian $H = \sum_x h_x$ such as the SYK model. Each term in the Hamiltonian is taken to be bounded, $\|h_x\| \leq \mathcal{E}$. We consider the moments and the Lanczos coefficients generated from a simple operator O (for example, a single Majorana operator in the SYK model). Defining $l_x = [h_x, \cdot]$, the n -th power of the Liouvillian is

$$\mathcal{L}^n |O\rangle = \sum_{x_1, \dots, x_n} l_{x_n} l_{x_{n-1}} \dots l_{x_1} |O\rangle. \quad (23)$$

Each application of l_{x_k} will increase the size of the operator by at most q , so the largest size of $l_{x_k} \dots l_{x_1} |O\rangle$ is $kq + 1$. Here, the size of a given operator refers to the number of elementary operators, such as a single Majorana operator ψ in the SYK model, contained in that operator. In order to have a nonzero term $l_{x_{k+1}} l_{x_k} \dots l_{x_1} |O\rangle$, $h_{x_{k+1}}$ and $l_{x_k} \dots l_{x_1} |O\rangle$ should have a nonvanishing overlap. For each nonvanishing term $l_{x_k} \dots l_{x_1} |O\rangle$, applying \mathcal{L} will lead to at most $2(kq + 1)N^{q-1}$ nonvanishing terms. As a result, the total number of nonvanishing terms of type $\mathcal{L}^n |O\rangle$ is bounded,

$$\prod_{k=1}^n 2((k-1)q + 1)N^{q-1} < (2qN^{q-1})^n n!. \quad (24)$$

Importantly, the number of nonvanishing terms increases as a factorial of n . Moreover, each individual term $l_{x_n} \dots l_{x_1} |O\rangle$ is bounded by $\|l_{x_n} \dots l_{x_1} |O\rangle\| \leq (2\mathcal{E})^n$. So the moment is bounded by

$$\mu_{2n} = \|\mathcal{L}^n O\|^2 \leq (2\mathcal{E})^{2n} (2qN^{q-1})^{2n} (n!)^2 < (4N^q \mathcal{E})^{2n} (n!)^2. \quad (25)$$

Thus, according to the bound between the moments and the Lanczos coefficients (21),

$$\prod_{k=1}^n b_k^2 \leq \mu_{2n} < (4N^q \mathcal{E})^{2n} (n!)^2, \quad (26)$$

the Lanczos coefficients can grow asymptotically $1 \ll k < N/q$ at most linearly, i.e., $b_k \propto k^\delta$, $\delta \leq 1$,

However, when the size of $\mathcal{L}^n |O\rangle$ is greater than N , which occurs when $n \geq N/q$, we can improve the bound as follows. If $l_{x_k} \dots l_{x_1} |O\rangle$ has size N , applying \mathcal{L} will lead to at most $2N^q$ nonvanishing terms. As a result, when $n \geq N/q$, the total number of nonvanishing terms in $l_{x_k} \dots l_{x_1} |O\rangle$ is

$$(2qN^{q-1})^{N/q} (N/q)! (2N^q)^{n-q/N} < (N/q)! (2N^q)^n. \quad (27)$$

In contrast to the situation when $n < N/q$, the number of nonvanishing terms now increase at most exponentially with n . The moments are bounded by

$$\mu_{2n} \leq (2\mathcal{E})^{2n} ((N/q)!)^2 (2N^q)^{2n} = ((N/q)!)^2 (4N^q \mathcal{E})^{2n}. \quad (28)$$

The Lanczos coefficients are bounded by the relation

$$b_{N/q+1}^2 \cdots b_n^2 \leq \frac{\mu_{2n}}{b_1^2 \cdots b_{N/q}^2} = \frac{((N/q)!)^2 (4N^q \mathcal{E})^{2(N/q)}}{b_1^2 \cdots b_{N/q}^2} (4N^q \mathcal{E})^{2(n-N/q)}, \quad (29)$$

which implies that $\delta = 0$ for $n \gg N/q$. Combining above results, we have

$$b_n \leq \begin{cases} \frac{\lambda_L}{2} n, & 1 \ll n \ll N/q \\ \frac{\lambda_C}{2} N, & N/q \ll n \ll 2^N \end{cases}, \quad (30)$$

where λ_L is the Lyapunov exponent, and λ_C is a constant independent of n . The factor N in the second line is to capture the system size dependence of b_n at $n \gg N/q$, such that λ_C is independent of the system size (see the following). The Lanczos coefficients thus exhibit a linear-to-plateau behavior.

Now as mentioned previously, the late-time plateau of Lanczos coefficients was first discussed in [29] based on the ETH conjecture. Here, we provided an explicit proof of this plateau behavior of the Lanczos coefficients, which strengthens the results of [29]. As we now review, the ETH conjecture is still useful to give an estimate of the plateau value of Lanczos coefficients [29]. We continue to work in a Hilbert space of N Majorana fermions, so the total dimension is $2^{N/2}$. Using the Lehmann representation in the energy eigenbasis $|E_a\rangle$, the Green function and moments read

$$G(\omega) = \frac{1}{\text{Tr}[O^\dagger O]} \sum_{ab} 2\pi \delta(\omega - (E_a - E_b)) |O_{ab}|^2, \quad O_{ab} \equiv \langle E_a | O | E_b \rangle \quad (31)$$

$$\mu_{2n} = \int \frac{d\omega}{2\pi} \omega^{2n} G(\omega) = \frac{1}{\text{Tr}[O^\dagger O]} \sum_{a,b} (E_a - E_b)^{2n} |O_{ab}|^2. \quad (32)$$

According to ETH, the matrix elements O_{ab} can be approximated by a random matrix to high accuracy in the thermodynamic limit, i.e., $O_{ab} = A(E_a, E_a)\delta_{ab} + A(E_a, E_b)2^{-N/4}R_{ab}$, where $A(E_a, E_b)$ is a smooth function of energies, R_{ab} denote random matrix with zero mean and unit variance. If we assume $A(E_a, E_b) = A(0, 0)F(E_a - E_b)$ is a function of the energy difference only, then we have

$$\mu_{2n} = 2^{-N/2} \sum_{a,b} (E_a - E_b)^{2n} \frac{|A(E_a, E_b)|^2}{\sum_c |A(E_c, E_c)|^2} = 2^{-N} \sum_{a,b} (E_a - E_b)^{2n} |F(E_a - E_b)|^2 \approx (N\mathcal{E})^{2n} \quad (33)$$

where we have implicitly averaged over the random matrix R_{ab} . The moment μ_{2n} is dominated by the largest energy difference between two many-body energy eigenvalues at large n . This implies $b_n \approx N\mathcal{E}$ at $n \gg N$, namely, the plateau value of Lanczos coefficient is proportional to the system size N .

The linear-to-plateau behavior of Lanczos coefficients in turn implies that, in a chaotic system, the average K-complexity of a simple Heisenberg operator will show exponential-to-linear growth,

$$C_K(t) \approx \begin{cases} e^{\lambda_L t}, & t_d \ll t \ll t_* \\ \lambda_C N t, & t_* \ll t \end{cases} \quad (34)$$

where λ_L and λ_C are constants, and $t_d = \lambda_L^{-1}$, $t_* = \lambda_L^{-1} \log N/q$ are the dissipation time and the scrambling time, respectively.

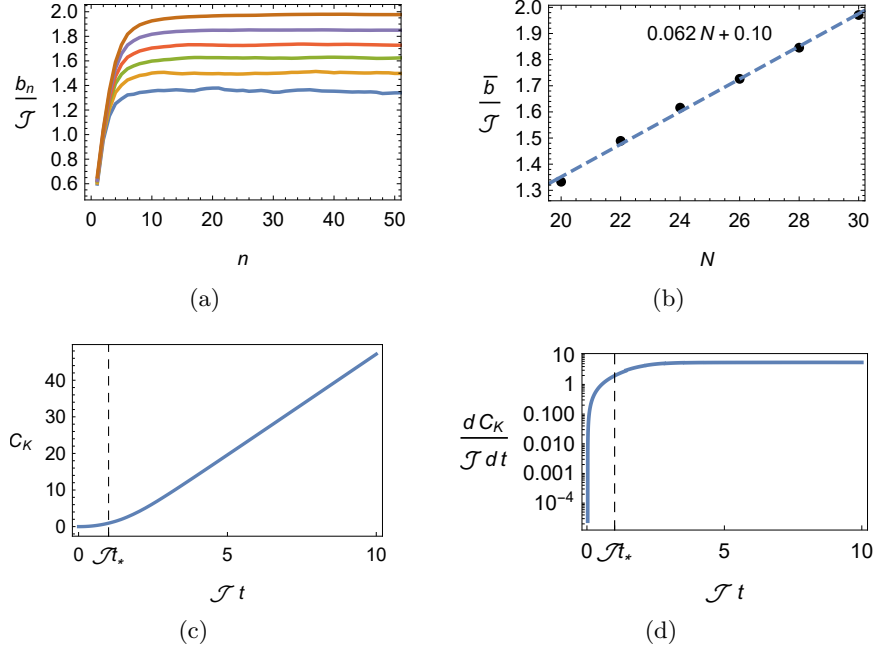


FIG. 2. (a) The Lanczos coefficient of the SYK model. The curves from the bottom to the top correspond to $q = 4$ and $N = 20, 22, 24, 26, 28, 30$, respectively. (b) The plateau value of the Lanczos coefficient at different N . \bar{b} given by the plateau value of the Lanczos coefficient $n > N/q$. The dashed line is fitted by a linear function, showing that the plateau value is proportional to N . (c) The K-complexity of the Heisenberg operator $\sqrt{2}\psi_1(t)$ in the SYK model. We use the parameters $q = 4$ and $N = 30$. (d) The time derivative of the K-complexity shown in (c). The scrambling time is denoted by t_* . Due to the small system size, the exponential growth is not obvious.

C. K-complexity growth of operators in the SYK model

We now consider the example of SYK in detail. Our goal is to demonstrate the expectations (34) explicitly. Once again, the SYK Hamiltonian is defined as

$$H = \frac{i^{\frac{q}{2}}}{q!} \sum_{j_1, \dots, j_q} J_{j_1, \dots, j_q} \psi^{j_1} \dots \psi^{j_q}, \quad \overline{J_{j_1, \dots, j_q}^2} = \frac{(q-1)! J^2}{N^{q-1}} = \frac{2^{q-1} (q-1)! \mathcal{J}^2}{q N^{q-1}}. \quad (35)$$

where the Majorana fermions satisfy $\psi_j^\dagger = \psi_j$, and $\{\psi_i, \psi_j\} = \delta_{ij}$. Exponential growth of K-complexity at early time in the SYK model has been obtained analytically in the large- q limit and numerically by solving the Schwinger-Dyson equation (see Appendix B in [28]). At large q , the operator wave function of a single Majorana fermion at time t is

$$\phi_n(t) = \sqrt{\frac{2}{nq}} \tanh^n \mathcal{J}t, \quad n \geq 1, \quad (36)$$

leading to exponential growth of K-complexity at early time,

$$C_K(t) = \sum_{n=1}^{\infty} n |\phi_n(t)|^2 = \frac{1}{q} (\cosh 2\mathcal{J}t - 1), \quad (37)$$

where the summation over the basis can be extended to infinity because we work at finite time with $N \rightarrow \infty$. The exponential growth exponent is $2\mathcal{J}$, consistent with the Lyapunov exponent at infinite temperature.

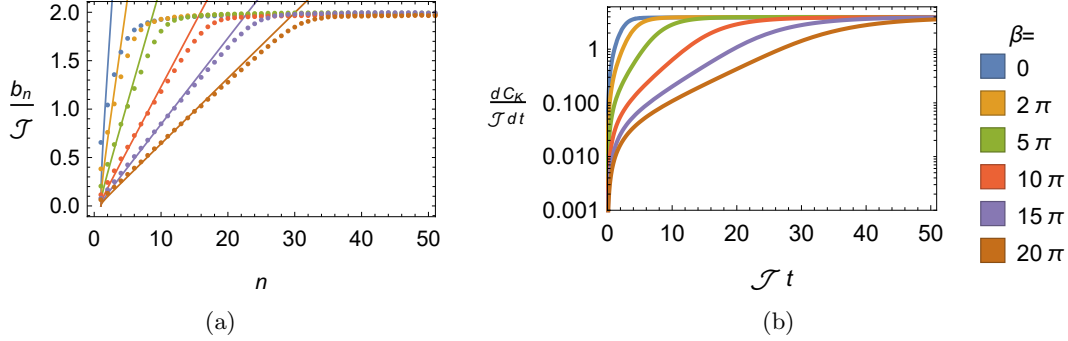


FIG. 3. (a) The Lanczos coefficient of the SYK model at different temperatures. The slope of the solid line is determined by $2\alpha(\beta)$. We use the parameters $N = 30, q = 4, \mathcal{J} = 1$. (b) The K-complexity growth of a single Majorana fermion at different temperature.

In getting (37), the large- N Wightman correlation function is used, but this only works for the K-complexity before the scrambling time. After the scrambling time, we expect a linear growth of K-complexity. To verify this conjecture, we choose $O = \sqrt{2}\psi_1$, and calculate the Lanczos coefficients numerically. For practical purposes, we can truncate the Krylov space at some $n_{\max} \gg 1$ and still capture the dynamics for a finite time related to n_{\max} . In Fig. 2(a), we plot the Lanczos coefficients for different choices of N , with all showing plateau behavior in the regime $n > N/q$. Moreover, the value of the plateau is proportional to the system size N , which is shown in Fig. 2(b). The K-complexity and its time derivative are calculated by solving the Schrödinger equation (10) for $q = 4$ and $N = 30$, with the results shown in Fig. 2(c) and 2(d). At late times, $t \gg t_* = \lambda_L^{-1} \log N/q$, the K-complexity grows linearly as expected. Due to the small number of qubits we simulate, $N/2 = 15$, the scrambling time is quite small, so the early time exponential regime is not manifest.

So far, we considered only the infinite temperature case. One way to generalize K-complexity to finite temperature is to consider the corresponding PETS $|O_\beta(\theta)\rangle$ at temperature $1/\beta$. This generalization is essentially equivalent to a change of definition of the inner product,

$$\langle O_1 | O_2 \rangle_\beta = \text{Tr}[e^{-\frac{\beta H}{2}(1+\frac{2\theta}{\pi})} O_1^\dagger e^{-\frac{\beta H}{2}(1-\frac{2\theta}{\pi})} O_2]. \quad (38)$$

For generic operator position θ , we have not been able to analytically obtain the Lanczos coefficients from the autocorrelation function. Nevertheless, for the special case $\theta = 0$, Ref. [28] obtained an analytic result at large q prior to the scrambling time. We briefly review their analytic results at short times (see Appendix A, and also the Appendix B in [28] for more details), and present a numerical evaluation valid at late times.

The moments are now related to the finite temperature Wightman correlation function,

$$G(t) = \frac{\text{Tr}[\rho^{1/2} O \rho^{1/2} O(t)]}{\text{Tr}[\rho^{1/2} O \rho^{1/2} O]}, \quad \rho = e^{-\beta H}, \quad \mu_{2n} = i^{2n} \frac{d^{2n}}{dt^{2n}} G(t)|_{t=0}, \quad (39)$$

Using the large- q Wightman correlation function at finite temperature $\beta > 0$ (Appendix A), we get the generalized K-complexity at early times,

$$C_K(t) = \sum_{n=1}^{\infty} n |\phi_n(t)|^2 = \frac{1}{q} (\cosh 2\alpha t - 1), \quad \alpha = \mathcal{J} \cos \frac{\alpha\beta}{2} \rightarrow \begin{cases} \mathcal{J}, & \mathcal{J}\beta \ll 1 \\ \pi/\beta, & \mathcal{J}\beta \gg 1 \end{cases}. \quad (40)$$

The exponential growth rate is given by 2α , which is equal to the Lyapunov exponent $\lambda_L = 2\alpha$ at large q [2].

The analytic wavefunction from the large- q Wightman correlation function also allows us to compute moments of \mathcal{C}_K operator. To do that, we can introduce the generating function of K-complexity, i.e.,

$$\langle e^{\mu \mathcal{C}_K} \rangle = 1 + \frac{4}{q} \log \operatorname{sech} \alpha t + \sum_{n=1}^{\infty} e^{\mu n} \frac{2}{nq} \tanh^{2n} \alpha t = (1 + (1 - e^\mu) \sinh^2 \alpha t)^{-2/q}, \quad (41)$$

$$F(\mu) = \log \langle e^{\mu \mathcal{C}_K} \rangle, \quad \langle (\mathcal{C}_K - C_K)^n \rangle = \frac{\partial^n}{\partial \mu^n} F(\mu) \Big|_{\mu=0}. \quad (42)$$

The n -th moment is given by taking n -th derivative of the generating function, but we will restrict ourselves to the average K-complexity. It would be interesting to explore the holographic duality of such an generating function in the future.

We also obtain the Lanczos coefficient at large $n \gg N$, as shown in Fig. 3(a), which show a similar linear-to-plateau pattern. The slope of the linear function in the Lanczos coefficient gets smaller at lower temperature, because the dynamics is slower, reflecting the decrease of the Lyapunov exponent $\lambda_L = 2\alpha$ with temperature. The ETH estimate applied to the operator O_β leads to $(O_\beta)_{ab} = A(E_a, E_a) \delta_{ab} + A(E_a, E_b) 2^{-N/2} R_{ab}$ with $A(E_a, E_b) = A(0, 0) F(E_a - E_b) e^{-\beta(E_a + E_b)/2}$. Similar to (33), $\mu_{2n} \sim (N\mathcal{E})^{2n}$ for $n \gg N$. As a result the plateau value of the Lanczos coefficient remains unaffected. The time derivative of K-complexity growth for various temperatures is plotted in Fig. 3(b), where the slope of the late-time linear growth is independent from the temperature, and the early-time exponential growth region expands due to the decrease of the Lyapunov exponent at finite temperatures.

III. HOLOGRAPHIC COMPLEXITY IN THE JT GRAVITY

A. Partially entangled thermal state in JT gravity

We now carry out corresponding calculations in JT gravity using complexity-volume duality. First, recall the setup of JT gravity. For a holographic conformal field theory, the bulk representation of the PETS state is a half disk with an operator inserted on its boundary [11, 13]. We assume that the dual bulk theory is JT gravity [19] with a matter field χ (the bulk field dual to operator O) coupling only to the metric,

$$I = I_{\text{bdy}}[g, \phi] + I_M[g, \chi], \quad (43)$$

$$I_{\text{bdy}}[g, \phi] = -\frac{\phi_0}{16\pi G_N} \left[\int \sqrt{g} R + 2 \int_{\partial} K \right] - \frac{1}{16\pi G_N} \left[\int d^2x \phi \sqrt{g} (R + 2) + 2 \int_{\partial} \phi_b K \right], \quad (44)$$

where G_N is the Newton's constant and g , R , K , ϕ , and ϕ_b refer to the metric, scalar curvature, extrinsic curvature, dilaton field and its value on the boundary, respectively. We require that the constant $\phi_0 \gg \phi$. The first term is purely topological. Because of the linear coupling to the dilaton field, the metric in the bulk is localized to AdS_2 , $ds^2 = \frac{d\tau^2 + dz^2}{z^2}$ (in this section, we work in Euclidean signature). So, the remaining dynamics of the metric are on the boundary. The boundary conditions are

$$g|_{\text{bdy}} = \frac{1}{\epsilon^2} d\tau^2, \quad \phi_b = \frac{\phi_r}{\epsilon}, \quad (45)$$

where ϕ_r is chosen to be a constant and τ is the imaginary time of the boundary theory. The remaining dynamics governed by the last term of (44) can be effectively reduced to the time

reparametrization field $\tilde{\tau} = f(\tau)$ at the boundary [19], which is governed by the Schwarzian action,

$$I_{\text{bdy}}[f] = -\frac{\phi_r}{8\pi G_N} \int_0^\beta d\tau \text{Sch}(f(\tau), \tau), \quad (46)$$

$$\text{Sch}(f(\tau), \tau) = -\frac{1}{2} \left(\frac{f''}{f'} \right)^2 + \left(\frac{f''}{f'} \right)'. \quad (47)$$

We assume that the inserted operator O is a single trace operator with scaling dimension Δ and the dual matter field χ vanishes in vacuum. The dimensionless inner product of the PETS becomes [11]

$$\epsilon^{2\Delta} \frac{\langle O_\beta(\theta) | O_\beta(\theta) \rangle}{\langle \mathbb{1}_\beta | \mathbb{1}_\beta \rangle} = \epsilon^{2\Delta} \langle O(\tau) O(\tau') \rangle_\beta = \frac{\delta^2 \int Df e^{-I_{\text{bdy}}[f] - I_M[f, \chi]} \Big|_{\chi=0}}{\delta\chi(X) \delta\chi(X')} \quad (48)$$

$$= \int Df \left(\frac{\epsilon^2 f'(\tau) f'(\tau')}{[f(\tau) - f(\tau')]^2} \right)^\Delta e^{-I_{\text{bdy}}} \approx \int Df \cosh^{-\Delta} D(X, X') e^{-I_{\text{bdy}}}, \quad (49)$$

$$\tau = \frac{\beta}{4} \left(1 + \frac{2\theta}{\pi} \right), \quad \tau' = -\frac{\beta}{4} \left(1 - \frac{2\theta}{\pi} \right), \quad (50)$$

where $X(X')$ denotes the point on the boundary and time $\tau(\tau')$, and $D(X, X')$ denotes the geodesic distance between the two points X and X' .

Operator insertions in JT gravity can be mapped to particles moving in a background AdS_2 with a uniform magnetic field [49]. The action is equivalent to

$$I = M \int d\tau \sqrt{h} - \frac{\phi_b}{8\pi G_N} \int d\tau \sqrt{h} K + \Delta \ln \cosh D(X, X') \equiv ML - QA + \mu L_\mu, \quad (51)$$

$$L = \frac{\beta}{\epsilon}, \quad Q = \frac{\phi_b}{8\pi G_N}, \quad \mu = \Delta, \quad L_\mu \approx D(X, X'), \quad (52)$$

where in the first step we have introduced a Lagrange multiplier M to fixed the boundary length L , and in the second step we have used the Gauss-Bonnet theorem (we neglect the unimportant constant 2π), $\int d\tau \sqrt{h} K = -\frac{1}{2} \int dx^2 \sqrt{g} R + 2\pi = A + 2\pi$, where we use $R = -2$ and A denotes the area enclosed by the boundary. Now it is apparent that the action is equivalent to a particle with charge Q and mass M moving in a hyperbolic space, where L is the length of the world line and A denotes the area enclosed by the world line. The action μL_μ describes a neutral particle, in which L_μ and μ are the world line length and the mass of the inserted particle, respectively. We call it the inserted particle because it describes the operator insertion. Several coordinate systems are convenient going forward, as summarized in Appendix B.

Throughout we assume a low energy limit and a classical limit $Q \gg L \gg 1$. In this situation, the world line length of the boundary particle is fixed, while its mass M is determined by the constraints. The parameters in the problem are thus Q , L , and μ . We also need to connect the world lines between the boundary particle, and the inserted particle according to the inserted position θ . By measuring them in units of the AdS radius, L , Q , and μ are rendered dimensionless.

To prepare the PETS, it is convenient to use an embedding space, $-(Y^{-1})^2 + (Y^0)^2 + (Y^1)^2 = -1$ with the metric $ds^2 = -(dY^{-1})^2 + (dY^0)^2 + (dY^1)^2$. The theory with both boundary particles and the inserted particle has an $SL(2)$ symmetry, and the equations of motion are dictated by the $SL(2)$ charges. In the rest frame of the matter particle, we make the following ansatz for the $SL(2)$ charges,

$$Z_i^a = \frac{Q}{\cosh r_i} (s_i \cosh \rho_i, 0, -\sinh \rho_i), \quad Z_\mu^a = (0, 0, -\mu), \quad s_{L,R} = -1, 1, \quad i = L, R. \quad (53)$$

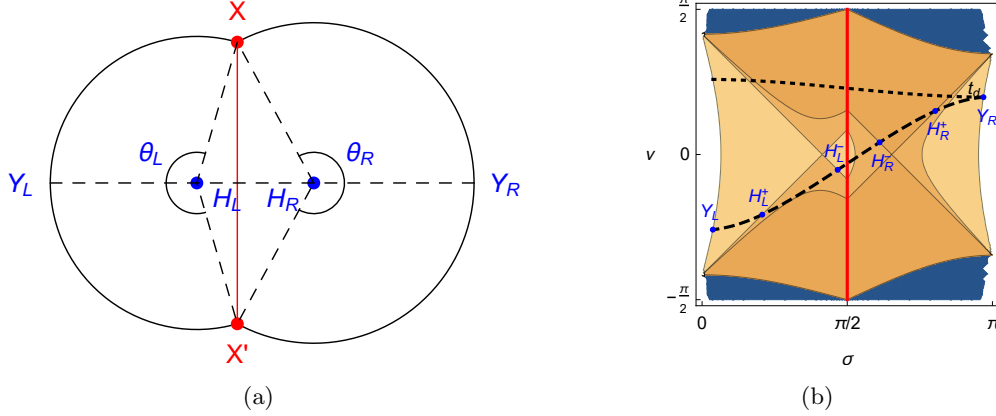


FIG. 4. (a) A schematic trajectory of boundary particles in hyperbolic space. The two segments and the vertical line represent the world lines of the two boundary particles and the inserted particle. The true horizon is point H_R . (b) The configuration of the dilaton field in the global coordinate of AdS_2 with the operator insertions. The parameters are $Q = 100$, $L = 30$, $\mu = 20$ and $\theta = \pi/20$. We plot the geodesics of $C_V(-t_d, t_d)$ (dashed) and $C_V(t_d, t_d)$ (dotted). These geodesics intersect the left boundary, left-outer horizon, left-inner horizon, right-inner horizon, right-outer horizon, and right boundary at points $\{Y_L, H_L^+, H_L^-, H_R^-, H_R^+, Y_R\}$.

where Q is the charge of boundary particles (note that the inserted particle is neutral), and r_i and ρ_i are constants determined by the equation of motion. The masses of boundary particles are related to r_i by $-Z_i \cdot Z_i = Q^2 - M_i^2$, more explicitly,

$$M_i^2 = Q^2 \tanh^2 r_i. \quad (54)$$

And μ is the mass of the inserted particle, which is related to the scaling dimension of O . Invariance under $SL(2)$ symmetry requires a conservation law,

$$Z_R + Z_L + Z_\mu = 0. \quad (55)$$

The equations of motion are also considerably simplified by the conservation law, and are given by

$$Z_R \cdot Y_R = -Q, \quad Z_L \cdot Y_L = Q, \quad Z_\mu \cdot Y_\mu = 0, \quad (56)$$

where Y_L and Y_R are the trajectories of the left and right boundary particles, respectively, and Y_μ is the trajectory of the inserted particle. In Rindler coordinates, the trajectories of the two boundary particles are

$$Y_i(\varphi) = e^{-s_i \rho_i T_2} (\cosh r_i, \sinh r_i \sin \varphi, \sinh r_i \cos \varphi)^T, \quad T_2 = \begin{pmatrix} 0 & 0 & 1 \\ 0 & 0 & 0 \\ 1 & 0 & 0 \end{pmatrix}. \quad (57)$$

Schematic trajectories for these particles are shown in Fig. 4(a); the two segments are world lines of the left and right boundary particles with centers H_L and H_R , respectively. The red line is the inserted particle. The segments are associated with angles θ_i which satisfy

$$\tanh \rho_i = -\tanh r_i \cos \frac{\theta_i}{2}, \quad i = L, R, \quad (58)$$

because the three trajectories join at X and X' . The length of the world lines of two boundary particles are fixed by

$$\theta_i \sinh r_i = \frac{L}{2} \left(1 + s_i \frac{2\theta}{\pi} \right), \quad (59)$$

which also enforces the total length to be L . With these equations, we can solve for θ_i and r_i in terms of the charges and masses of the particles.

The dilaton field can be determined from its equation of motion. At point Y , one has

$$\frac{\phi}{8\pi G_N} = \begin{cases} Z_L \cdot Y, & Y^1 < 0 \\ -Z_R \cdot Y, & Y^1 > 0 \end{cases}. \quad (60)$$

Figure 4(b) shows the configuration of the dilaton field for the PETS in global coordinates for AdS_2 . When the centers H_L and H_R are on the both sides of the trajectory of the inserted particle in Euclidean AdS_2 , as shown in Fig. 4(a), the dilaton field reaches extremal values at the two points. We will call them horizons H_L, H_R although only the one with the smaller value of dilaton is the true horizon [11]. Each of the horizons extends along a light cone in Lorentzian AdS_2 , as shown in Fig. 4(b). We will call the left(right)-going light cone of the left horizon as the left-outer(inner) horizon, and the right(left)-going light cone of the right horizon as the right-outer(inner) horizon.

Using the conservation law (55) and the constraints (58,59), the $SL(2)$ charges of the boundary particles can be obtained numerically. One can also get analytic solutions perturbatively in $\frac{\mu L}{Q} \ll 1$,

$$r_i = r - \frac{2 + (\pi + 2\theta s_i) \tan \theta}{4\pi^2} \frac{\mu L}{Q}, \quad (61)$$

where $\sinh r = \frac{L}{2\pi}$ is the unperturbed radius.

However, at $\theta = \frac{\pi}{2}$, the expansion in (61) breaks down. To get a meaningful result, one can regularize to $\theta = \frac{\pi}{2} - \delta$, then expand first in $\delta \rightarrow 0$ and then in $\frac{\mu L^2}{Q} \ll 1$. The result is

$$r_R = r, \quad r_L = r - \frac{1}{4\pi^2} \frac{\mu L^2}{Q}. \quad (62)$$

In this case, the expansion parameter is $\frac{\mu L^2}{Q}$ which differs from the parameter $\frac{\mu L}{Q}$ at generic θ . This reflects the non-commutativity of the two expansions in $\delta = 0$ limit.

B. Holographic complexity growth of the Heisenberg operator

We define the holographic complexity $C_V(t)$ of the Heisenberg operator as the holographic complexity of the corresponding PETS. In two-dimensional spacetime, the CV conjecture [21] states that the holographic complexity is proportional to the geodesic distance D between the boundary points at times t_L and t_R in Lorentzian signature. It is approximated by [41]

$$C_V(t_L, t_R) \approx \frac{\phi_0}{G_N} D(Y_L(\pi - iu_L), Y_R(iu_R)), \quad u_i = \frac{2\pi t_i}{\beta_i}, \quad \beta_i = \frac{\pi + 2\theta s_i}{\theta_i} \beta, \quad (63)$$

where ϕ_0 dominates the cross-section. The geodesic distance $D(Y_1, Y_2)$ between points Y_1 and Y_2 can be evaluated by the inner product in the embedding space, $\cosh(D(Y_1, Y_2)) = -Y_1 \cdot Y_2$. Finally, letting $\tilde{C}_V = \frac{G_N}{\phi_0} C_V$, we have

$$\begin{aligned} \cosh \tilde{C}_V(t_L, t_R) &= \cosh(\rho_L + \rho_R) (\cosh r_L \cosh r_R + \sinh r_L \sinh r_R \cosh u_L \cosh u_R) \\ &\quad - \sinh(\rho_L + \rho_R) (\sinh r_L \cosh r_R \cosh u_L + \cosh r_L \sinh r_R \cosh u_R) \\ &\quad + \sinh r_L \sinh r_R \sinh u_L \sinh u_R. \end{aligned} \quad (64)$$

Consider first the case with $-t_L = t_R = t$. The choice of opposing directions of time evolution corresponds to the Heisenberg evolution of operators, $U(t)^\dagger O_\beta(\theta) U(t)$. Without the inserted

particle, $\mu = 0$, the bulk is unperturbed and recovers the Rindler patch of AdS_2 , $\rho_L + \rho_R = 0$, $r_L = r_R = r$ and $-u_L = u_R = \frac{2\pi t}{\beta}$. The complexity is $C_V[\mathbb{1}_\beta] = 2\phi_0 r/G_N$, which is independent of time because of boost symmetry of TFD state.

In the light operator limit, $\mu L \ll Q$, and considering $|\theta| \neq \pi/2$, the perturbed solution (61) can be used to get the geodesic length,

$$\cosh \tilde{C}_V(-t, t) = \begin{cases} \frac{e^{2r}}{2} \left(1 + \frac{\pi \sec \theta \cosh u - (2+2\theta \tan \theta) \mu L}{2\pi^2} \frac{\mu L}{Q} \right), & t_d \ll t \ll t_* \\ \frac{1}{2} \left(\frac{\sec \theta}{8\pi} \frac{\mu L}{Q} e^{r+u} \right)^2, & t \gg t_* \end{cases}, \quad u = \frac{2\pi}{\beta} t \quad (65)$$

where $r \sim \ln L$, and the dissipation time and the scrambling time are, respectively,

$$t_d = \frac{\beta}{2\pi}, \quad t_* = \frac{\beta}{2\pi} \ln \frac{8\pi Q \cos \theta}{\mu L}. \quad (66)$$

At late time, we only need consider the leading time dependence in (64). The complexity grows exponentially at early time and linearly at late time,

$$\tilde{C}_V(-t, t) \approx \begin{cases} 2r + \frac{\sec \theta}{2\pi} \frac{\mu L}{Q} \cosh u, & t_d \ll t \ll t_* \\ 2 \log \left(\frac{\sec \theta}{8\pi} \frac{\mu L}{Q} \right) + 2r + 2u, & t \gg t_*, \end{cases} \quad (67)$$

The early time exponential growth has Lyapunov exponent $\lambda_L = 2\pi/\beta$, and at late time the linear growth rate of \tilde{C} is $\lambda_C = 4\pi/\beta$.

In the $\theta = \frac{\pi}{2}$ case, we use instead the perturbed solution (62), and expand the geodesic length in the limit $\delta \rightarrow 0$ and $\mu L^2 \ll Q$,

$$\cosh \tilde{C}_V(-t, t) = \begin{cases} \frac{e^{2r}}{2} \left(1 + \frac{\cosh u - 1}{4\pi^2} \frac{\mu L^2}{Q} \right), & t_d \ll t \ll t_* \\ \frac{1}{2} \left(\frac{1}{2\pi} \frac{1}{8\pi} \frac{\mu L^2}{Q} e^{r+u} \right)^2, & t \gg t_* \end{cases}, \quad u = \frac{2\pi}{\beta} t, \quad (68)$$

leading to the following complexity dynamics,

$$\tilde{C}_V(-t, t) \approx \begin{cases} 2r + \frac{1}{4\pi^2} \frac{\mu L^2}{Q} \cosh u, & t_d \ll t \ll t_* \\ 2 \log \left(\frac{1}{2\pi} \frac{1}{8\pi} \frac{\mu L^2}{Q} \right) + 2r + 2u, & t \gg t_* \end{cases}. \quad (69)$$

In particular, the qualitative behavior is not modified by the change in perturbation parameter and the Lyapunov exponent and late time exponent are still given by $\lambda_L = 2\pi/\beta$ and $\lambda_C = 4\pi/\beta$, respectively. It is also interesting to note that if one regularizes the infinity at $\frac{\pi}{2}$ by $\sec \frac{\pi}{2} \rightarrow \frac{L}{2\pi}$, then (65) can include the case $\theta \rightarrow \frac{\pi}{2}$ as well.

These analytic results are also consistent with a numerical evaluation of the shown in Fig. 5. The numerical solution indeed shows complexity growing exponentially at first and linearly after the scrambling time.

Now, when H_L, H_R are on both sides of the trajectory of the inserted particle, the geodesic giving the complexity crosses the left/right-inner/outer horizons at points $\{H_L^+, H_L^-, H_R^-, H_R^+\}$ from left to right, as shown in Fig. 4(b). Combining with the two points $\{Y_L, Y_R\}$ on the boundaries, they divide the complexity geodesic into five intervals. We plot the contributions of these intervals to the complexity in Fig. 5 in the light operator limit. The growth of complexity is mainly due to the growth of the length of the geodesic distances inside the black hole interiors $D(H_L^+, H_L^-)$ and $D(H_R^-, H_R^+)$. Note in particular the similarity between Fig. 5 and the K-complexity in Figs. 2(c), 2(d).

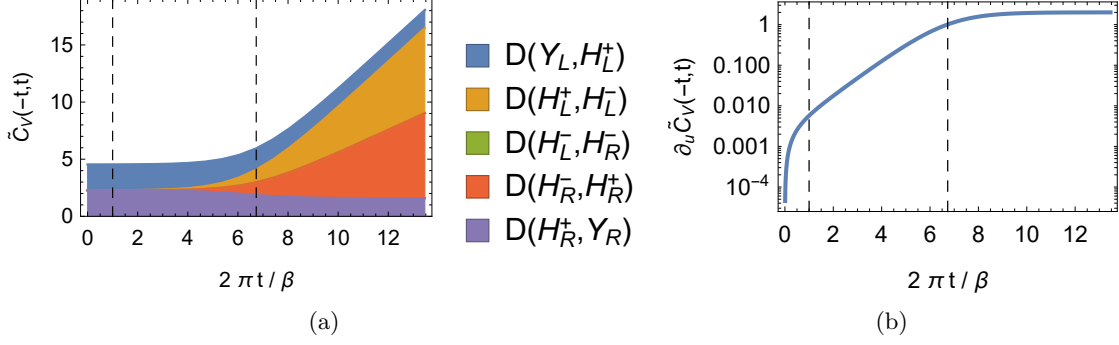


FIG. 5. (a) The complexity growth of a light Heisenberg operator, where the contributions from the intervals between points $\{Y_L, H_L^+, H_L^-, H_R^-, H_R^+, Y_R\}$ are shown, where the contribution from $D(H_L^-, H_R^-)$ is too small to be seen. (b) The time derivative of the complexity growth. The two dashed lines indicate the dissipation time t_d and the scrambling time t_* in (66). The parameters are $Q = 100$, $L = 30$, $\theta = 0$, and $\mu = 0.1$.

To compare with the SYK model, we identify $\epsilon = 1/\mathcal{J}$. Then the parameters of the JT gravity and the SYK model are related by

$$Q = \alpha_S N, \quad L = \beta \mathcal{J}, \quad \mu = \frac{1}{q}, \quad \frac{\phi_0}{4G_N} = sN, \quad (70)$$

α_S and s are some numerical constants. At the large q limit, $\alpha_S = \frac{1}{4q^2}$ and $s = \frac{1}{2} \ln 2$ [2]. Based on (40), if the boundary length segments are subtracted from the holographic complexity, we get the following equality in the conformal limit,

$$\frac{\Delta C_V(t)}{L} = \frac{\alpha_C}{q} (\cosh \frac{2\pi t}{\beta} - 1) = \alpha_C C_K(t), \quad \alpha_C = \frac{2s}{\pi \alpha_S}, \quad t_d < t < t_*. \quad (71)$$

where we have set $\theta = 0$ for comparison since the PETS used in K-complexity corresponds to $\theta = 0$. Note that the scrambling time for K-complexity, $\frac{\beta}{2\pi} \log \frac{N}{q} \frac{\mathcal{J}}{\alpha} \approx t_*(1 + O[(\log N)^{-1}])$, is approximately equal to the scrambling time of the holographic complexity in the large N limit. It is also interesting to compare the rate of complexity growth for both K-complexity and holographic complexity. In the conformal limit, the following equations hold after the scrambling time,

$$\frac{d \log C_V(-t, t)}{dt} = \frac{d \log C_K(t)}{dt}, \quad t > t_d. \quad (72)$$

At this level, the K-complexity defined in (12) thus gives a microscopic counterpart of holographic complexity.

If two sides are evolved in the same time direction, then the complexity will grow linearly at first since the complexity of the time evolution operator U will dominate over the simple operator O . The geodesic length and complexity are

$$\cosh D(t, t) = \frac{e^{2r}}{2} \cosh^2 u \left(1 + \frac{\pi \sec \theta \operatorname{sech} u - (2 + 2\theta \tan \theta) \frac{\mu L}{Q}}{2\pi^2} \right), \quad (73)$$

$$\tilde{C}_V(t, t) \approx 2r + 2u, \quad t \gg t_d, \quad u = \frac{2\pi t}{\beta}. \quad (74)$$

At late time, this growth is equivalent to the late-time linear growth of the complexity in simple Heisenberg operators. This is because the Heisenberg operator becomes complicated after the scrambling time, and the Heisenberg evolutions at two sides become mostly uncorrelated.

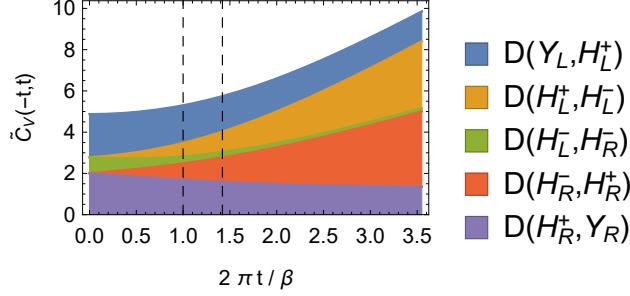


FIG. 6. The complexity growth of a heavy Heisenberg operator. The parameters are $Q = 100$, $L = 30$, $\mu = 20$ and $\theta = \pi/20$.

Another interesting limit is the heavy operator limit. When $\mu = 2Q$, the two segments in Fig. 4(a) become two tangent thermal circles now with inverse temperatures $\beta_i = \frac{\pi+2\theta s_i}{2\pi} \beta$, respectively. The operator O is already complicated initially, and there is not a large separation between scrambling time and dissipation time, as shown in Fig. 6. In this limit, the complexity approximately decomposes into the complexities of two wormholes separately,

$$\begin{aligned} \tilde{C}_V(t_L, t_R) &\approx 2 \ln \left(\frac{\beta_L}{\pi\epsilon} \cosh \frac{\pi t_L}{\beta_L} \right) + 2 \ln \left(\frac{\beta_R}{\pi\epsilon} \cosh \frac{\pi t_R}{\beta_R} \right) \\ &= \tilde{C}_V[e^{-(\frac{1}{2}\beta_L + it_L)H}] + \tilde{C}_V[e^{-(\frac{1}{2}\beta_R + it_R)H}]. \end{aligned} \quad (75)$$

This form exhibits quadratic growth when $t \ll t_d$ and linearly growth when $t \gg t_d$. The decomposition reflects the fact that the heavy operator O effectively cuts the wormhole into two shorter wormholes while creating a large interior, similar to a Python's lunch geometry [53], as shown in Fig. 4(b). The geodesic length at two wormholes grows with time independently with their own inverse temperature β_i .

IV. THE SIZE OF THE PARTIALLY ENTANGLED THERMAL STATE

A. The size from the SYK model

In this section we obtain some results for operator size and compare them to the preceding complexity results. The maximally entanglement state $|0\rangle$ defined in the doubled SYK Hilbert space satisfies $c^j |0\rangle = 0, \forall j$ where $c^j = (\psi_L^j + i\psi_R^j)/\sqrt{2}$. The size of an operator ψ in the SYK model can be defined as $n[\psi] = \langle \psi | \hat{n} | \psi \rangle / \langle \psi | \psi \rangle$, where the size operator is $\hat{n} = \sum_{j=1}^N (c^j)^\dagger c^j = N/2 + i \sum_j \psi_L^j \psi_R^j$ [8]. At large q and early time, the growth of size of operator $O_\beta(\theta + iu) = \sqrt{2}\psi_\beta^1(\theta + iu)$ is characterized by

$$\Delta \tilde{n}(t) = \frac{n[O_\beta(\theta + iu)] - n[\mathbb{1}_\beta]}{\delta_\beta} = \sec\left(\frac{\pi v}{2}\right) \sec(\theta v) \cosh\left(\frac{2\pi v}{\beta} t\right) - \frac{2 \tan\left(\frac{\pi v}{2}\right) (\theta v \tan(\theta v) + 1)}{\pi v + 2 \cot\left(\frac{\pi v}{2}\right)} \quad (76)$$

where $v = \alpha\beta/\pi$, $u = 2\pi t/\beta$, and the normalization factor $\delta_\beta = 2G(\frac{\beta}{2})$ is determined by $\Delta \tilde{n}(0) = 1$ when $\theta = \frac{\pi}{2}$. At late time, the exponential growth will slow and eventually vanish as the size approaches $\Delta \tilde{n}(\infty) = N/2$. More generally, one can obtain the generating function of size operator at arbitrary inserting angle θ , and it turns out the generating function of size operator agrees with that of K-complexity C.

Notice that, in the large q limit, the scrambling time obtained from both C_K and C_V is $t_* \sim \lambda_L^{-1} \ln(N/q)$ rather than $\lambda_L^{-1} \ln N$. So $\Delta \tilde{n}(t_*) = N/q$ rather than its saturation value $N/2$, which implies that $\Delta \tilde{n}(t_*)$ deviates from exponential growth before saturation. We will discuss this point in Appendix D.

B. The size derived from JT gravity

The size is related to the symmetries of AdS_2 in JT gravity. The $SL(2)$ generators $\tilde{B}, \tilde{E}, \tilde{P}$ in the dual AdS_2 are related to the operators in the two sites SYK model [16]

$$\hat{B} = \frac{\beta}{2\pi} (H_R - H_L), \quad (77)$$

$$\hat{E} = \frac{\beta}{2\pi} [H_R + H_L + \tilde{\mu} \hat{n} - \langle \mathbb{1}_\beta | (H_R + H_L + \tilde{\mu} \hat{n}) | \mathbb{1}_\beta \rangle], \quad (78)$$

$$\hat{P} = -i[\hat{B}, \hat{E}], \quad (79)$$

$$\text{where } \frac{\tilde{\mu}}{\mathcal{J}} = \frac{2\alpha_S}{\Delta\delta_\beta} \left(\frac{2\pi}{\beta\mathcal{J}} \right)^2. \quad (80)$$

For conciseness, we consider that the states are normalized. The normalized change of size can be written as

$$\begin{aligned} \Delta \tilde{n}(t) &= \frac{1}{\delta_\beta} [\langle O_\beta(\theta + iu) | \hat{n} | O_\beta(\theta + iu) \rangle - \langle \mathbb{1}_\beta | \hat{n} | \mathbb{1}_\beta \rangle] \\ &= \frac{1}{\tilde{\mu}\delta_\beta} \frac{2\pi}{\beta} \left[\langle O_\beta(\theta + iu) | (\hat{E} - \hat{B} - \frac{\beta}{\pi} H_L) | O_\beta(\theta + iu) \rangle + \frac{\beta}{\pi} \langle \mathbb{1}_\beta | H_L | \mathbb{1}_\beta \rangle \right] \\ &= \frac{\Delta\mathcal{J}}{2\alpha_S} \frac{\beta}{2\pi} \left[\langle O_\beta(\theta + iu) | (\hat{E} - \hat{B}) | O_\beta(\theta + iu) \rangle + \partial_\varphi \ln G \left(\frac{\beta}{2} \left(1 - \frac{2\theta}{\pi} \right); \beta \left(1 + \frac{\varphi}{\pi} \right) \right) \Big|_{\varphi=0} \right], \end{aligned} \quad (81)$$

where $G(\tau; \beta) = \text{Tr}[e^{-\beta H} O^\dagger(\tau) O] / \text{Tr}[e^{-\beta H}]$. Its time derivative is proportional to the momentum

$$\partial_t \Delta \tilde{n}(t) = \frac{\Delta\mathcal{J}}{2\alpha_S} \langle O_\beta(\theta + iu) | \hat{P} | O_\beta(\theta + iu) \rangle. \quad (82)$$

According [16], when we insert operators to the thermal circle at $\phi_t = \frac{\pi}{2} - \theta + iu$, $\phi_b = -\frac{\pi}{2} + \theta + iu$, the generators are

$$\begin{aligned} \frac{\langle O_\beta(\phi_t)^\dagger | (\hat{B}, \hat{P}, \hat{E}) | O_\beta(\phi_b) \rangle}{\langle O_\beta(\phi_t)^\dagger | O_\beta(\phi_b) \rangle} &= \frac{\Delta}{\sin \frac{\phi_-}{2}} \left(\cos \frac{\phi_-}{2}, -i \sin \frac{\phi_+}{2}, \cos \frac{\phi_+}{2} \right) = \frac{\Delta}{\cos \theta} (\sin \theta, \sinh u, \cosh u) \\ \text{where } \phi_- &= \phi_t - \phi_b = \pi - 2\theta, \quad \phi_+ = \phi_t + \phi_b = 2iu. \end{aligned} \quad (83)$$

At large q limit, we obtain

$$\Delta \tilde{n}(t) = \frac{\beta\mathcal{J}}{\pi^2} (-2 - \pi \tan \theta + \pi \sec \theta \cosh \frac{2\pi t}{\beta}), \quad (84)$$

which is equal to (76) from the SYK model at $\beta\mathcal{J} \gg 1$ limit.

C. Relation between the operator size and the complexity

We first discuss the relation between K-complexity and the size operator. At infinite temperature, the time derivative of K-complexity is proportional to the size at early times $t_d \ll t \ll t_*$. Relating (40) and (76), we find that

$$\frac{1}{2\mathcal{J}} \frac{dC_K(t)}{dt} \approx \frac{1}{q} \Delta \tilde{n}(t), \quad \beta \rightarrow 0. \quad (85)$$

Actually, the generating functions of K-complexity and size operator agree, as shown in Appendix C. For finite temperature and $\theta = 0$, the relation will be modified by a temperature dependent factor,

$$\frac{1}{2\mathcal{J}} \frac{dC_K(t)}{dt} \approx \frac{1}{q} \left(\cos^2 \frac{\pi v}{2} \right) \Delta \tilde{n}(t). \quad (86)$$

This relation may be extended to late times after the scrambling time. The linear growth of K-complexity at late times is proportional to the system size, i.e., $\frac{1}{2\mathcal{J}} \frac{dC_K(t)}{dt} \propto \frac{N}{2} = \Delta n(t)$ for $t \gg t_*$.

Now we consider the relation between the holographic complexity and the size operator. The size of an operator is linearly related to its out of time order correlator (OTOC) with Majorana fermions ψ_i [8]. From the geometric interpretation of effective theory [11, 54], we find the following relation between the size in the SYK model and the complexity in JT gravity at the limit $q \gg 1$, $N \gg \beta\mathcal{J} \gg 1$ and the early time,

$$\frac{\pi^2}{\beta\mathcal{J}} \frac{\Delta \tilde{n}[\psi_\beta^1(\theta + iu)]}{N/2} = -2 - 2\theta \tan \theta + \pi \sec \theta \cosh t = \frac{2\pi^2 Q}{\mu L} \frac{G_N}{\phi_0} (C_V[\psi_\beta^1(\theta + iu)] - C_V[1_\beta]) \quad (87)$$

which is valid under the dictionary (70). Combining it with the Epidemic relation $\frac{d}{dt} \Delta \tilde{n} = \lambda_L \Delta \tilde{n}$ at the Lyapunov regime [8], we find

$$\frac{1}{TS_0} \frac{dC_V}{dt} = \frac{\Delta \tilde{n}}{N/q}, \quad (88)$$

where entropy $S_0 = \frac{\phi_0}{4G_N} = sN$ and temperature $T = 1/\beta$.

V. CONCLUSION AND OUTLOOK

We calculated the complexity of a Heisenberg operator in both the SYK model and JT gravity. In the SYK model, we used the notion of K-complexity defined through the Krylov basis. One advantage of K-complexity is that it is uniquely determined by the reference operator and the Hamiltonian. In the JT gravity model, we used the CV conjecture to define the complexity. The simplicity of JT gravity allowed us to treat the problem of gravitational back-reaction by mapping it to motions of particles in a rigid hyperbolic space. We found that both complexities show an exponential-to-linear growth behavior. In particular, the two notions of complexity actually match up to a constant before the scrambling time. After the scrambling time, although the characteristic energy scales for the two complexities are different, they both show a linear growth with a slope proportional to system size. We also verified the relation between complexity growth and operator size before the scrambling time. The complexity can be used to capture the quantum dynamics at both short and long times.

It is worth noting the temperature dependence of the holographic complexity. For a generic insertion $\theta \neq \pm\pi/2$, the complexity is inversely proportional to the temperature, $C_V \propto (\beta/\epsilon) e^{2\pi t/\beta}$

before the scrambling time, and it is proportional to the temperature in the linear growth regime $C_V \propto (\phi_0/G_N)4\pi t/\beta$ after the scrambling time. The former is due to the fact that the inserted operator is perturbing the wormhole with temperature $1/\beta$, while the latter is due to the relation between the Lorentzian time and the Rindler time.

By contrast, the role of temperature is less clear in the context of computational complexity, so it is interesting to attempt to introduce temperature into the definition of computational complexity. For example, the temperature dependence of the holographic complexity means a simple identification of the circuit time and the Lorentzian time is not enough to set the complexities equal up to an overall constant. In our study, we generalized the K-complexity to finite temperature by considering the PETS at temperature $1/\beta$ as the reference state. This is essentially the same as a temperature-dependent inner product [28]. However, as we showed based on (71), such a generalization does not give a completely consistent identification between the two notions of complexity after scrambling time. By adjusting the overall normalization of one or the other, one could match the early or late time growth but not both. Hence, it is interesting to consider further refinements that might produce even more harmony between the two notions of complexity. Nevertheless, we emphasize that at the level of the rate of complexity growth, the identification between the notions works perfectly well at early and late time as in (72). This suggests that as far as the temperature dependence is concerned, the rate of complexity growth ratio and the related time scales have simpler holographic interpretation than the absolute value of complexity itself.

The CV proposal used in this paper only depends on the geometry and the dilaton. It is an open question that whether matter fields should have a direct contribution to the holographic complexity besides their indirect contribution via back-reaction on the metric. The answer to this question may be crucial for the complexity of heavy operators, such as (75). From the perspective of complexity-action (CA) conjecture [35, 36, 40–45], the action of the matter field along the trajectory of the inserted particle can directly contribute. We hope to explore this problem in the future.

It is also interesting to consider higher dimensional generalization of PETS and its gravity dual. For instance, in three dimensions, we may insert an end of world brane behind the horizon of an eternal black hole, corresponding to the geometry worked out in [55] in the context of an evaporating black hole. The holographic complexity in this case is then proportional to the volume of a two-dimensional maximal surface connecting the two boundaries. From the viewpoint of evaporating black holes, the geometry of the PETS in our study is effectively dual to a two-dimensional version of the entangled system consisted of the black hole and the auxiliary radiation [55, 56]. And the holographic complexity calculated here is the so-called unrestricted complexity for decoding the radiation [53].

ACKNOWLEDGEMENT

S. K. J. and B. S. are supported by the Simons Foundation via the It From Qubit Collaboration. Z. Y. X. is supported in part by the Natural Science Foundation of China under Grant No. 11875053 and by the National Postdoctoral Program for Innovative Talents BX20180318, funded by China Postdoctoral Science Foundation.

Appendix A: K-complexity in the SYK model at early times

We will summarize the Wightman correlation function and the K-complexity at early times (e.g. see Appendix B in [28] for more details). Using the large- q approximation, the imaginary

time correlation function at temperature β is given by

$$2\langle \mathcal{T}_\tau \psi(\tau) \psi(0) \rangle = 1 + \frac{2}{q} \log \frac{\alpha}{\mathcal{J} |\cos \alpha(\tau - \beta/2)|}, \quad \tau > 0, \quad \alpha = \mathcal{J} \cos \frac{\alpha\beta}{2}. \quad (\text{A1})$$

So, the Wightman correlation function is

$$G(t) = 1 + \frac{2}{q} \log \frac{1}{\cosh \alpha t}. \quad (\text{A2})$$

where we have properly normalize it by $G(0) = 1$. And accordingly the wavefunction of a simple Majorana fermion is [28]

$$\phi_n(t) = \sqrt{\frac{2}{nq}} \tanh^n \alpha t, \quad n \geq 1. \quad (\text{A3})$$

This leads to the exponential growth of K-complexity at early time,

$$C_K(t) = \sum_{n=1}^{\infty} n |\phi_n(t)|^2 = \frac{1}{q} (\cosh 2\alpha t - 1), \quad \alpha = \mathcal{J} \cos \frac{\alpha\beta}{2}. \quad (\text{A4})$$

Appendix B: Summary of coordinate systems

We summarize various coordinate systems used in the paper. We start with embedding coordinate. AdS_2 space can be embedded to

$$-Y_{-1}^2 - Y_0^2 + Y_1^2 = -1, \quad ds^2 = -dY_{-1}^2 - dY_0^2 + dY_1^2. \quad (\text{B1})$$

The global coordinate which we use to plot the perturbed AdS_2 spacetime is given by

$$Y^{-1} = \frac{\cos \nu}{\sin \sigma}, \quad Y^0 = \frac{\sin \nu}{\sin \sigma}, \quad Y^1 = \cot \sigma, \quad ds^2 = \frac{-d\nu^2 + d\sigma^2}{\sin^2 \sigma}. \quad (\text{B2})$$

The Lorentzian coordinate system is related to the embedded coordinate by

$$Y^{-1} = \frac{z}{2} \left[1 + \frac{1}{z^2} (1 - \tilde{t}^2) \right], \quad Y^0 = \frac{\tilde{t}}{z}, \quad Y^1 = \frac{z}{2} \left[1 - \frac{1}{z^2} (1 + \tilde{t}^2) \right], \quad ds^2 = \frac{-d\tilde{t}^2 + dz^2}{z^2}. \quad (\text{B3})$$

Furthermore, a possible Rindler coordinate is

$$Y^{-1} = \cosh r, \quad Y^0 = \sinh r \sinh \varphi, \quad Y^1 = \sinh r \cosh \varphi, \quad ds^2 = dr^2 - \sinh^2 \rho d\varphi^2. \quad (\text{B4})$$

Appendix C: Generating function for size at generic θ

The generating function of size can be obtained in the large- q limit. A simple generalization of [8] gives the generating function of size operator at generic angle θ ,

$$\begin{aligned} \langle e^{\mu \hat{n} / \delta_\beta} \rangle &= \frac{e^{\mu \left(\frac{\cos \alpha\beta/2}{\cos \alpha\beta\theta/\pi} \right)^{2/q}}}{\left[\cos \alpha\beta/2 \cos \alpha\beta\theta/\pi - (1 - e^{q\mu})(\cos \alpha\beta(1/2 - \theta/\pi) - 1)/2 + (1 - e^{q\mu}) \sinh^2 \alpha t \right]^{2/q}}, \\ Z(\mu) &= \log \langle e^{\mu \hat{n} / \delta_\beta} \rangle, \quad \left\langle \left(\frac{\hat{n} - \langle \hat{n} \rangle}{\delta_\beta} \right)^k \right\rangle = \frac{d^k}{d\mu^k} Z(\mu) \Big|_{\mu=0}, \\ \alpha/\mathcal{J} &= \cos \alpha\beta/2, \quad \delta_\beta = (\alpha/\mathcal{J})^{2/q}. \end{aligned} \quad (\text{C1})$$

At infinite temperature $\beta \rightarrow \infty$, the generating function reduces to

$$\langle e^{\mu \hat{n}} \rangle = \frac{e^\mu}{\left[1 + (1 - e^{q\mu}) \sinh^2 \mathcal{J}t\right]^{2/q}}, \quad (\text{C2})$$

which agrees exactly with that of K-complexity in (41) if one renormalizes the size by a factor of q since by each step the Liouvillian the size increases a constant amount q . Note that the generating function works prior to the scrambling time since we implement the large- q approximation.

Appendix D: About the scrambling time

In this paper, the scrambling time is defined as the time of the crossover between the exponential growth and the linearly growth of complexities. We will show that this scrambling time also appears in the growth of the size, *i.e.* the decay of the OTOC, which should slow down before saturation.

The Schwarizan theory (46) is able to capture the decay of OTOCs at both early time and late time. In Ref. [54], the OTOC $\langle B_{l_2}(\tilde{t}_1) A_{l_1}(\tilde{t}_2) B_{l_2}(t_1) A_{l_1}(t_2) \rangle$ corresponds to the gravitational scattering between the outgoing matter A and the infalling matter B near the horizon of the black hole with initial mass $m = \pi/\beta$. Semi-classically, assuming that the change in the mass of the black hole due to the matter is much smaller than m , and considering the small scaling dimensions $l_1, l_2 \approx 0$, one find that the time shift of the the outgoing matter A is

$$\tilde{t}_2 - t_2 \approx \frac{1}{\lambda_L} \ln \left(1 + 4\alpha C e^{\lambda_L(t_2 - t_1 - t_R)} \right), \quad (\text{D1})$$

where $C = \frac{\phi_r}{8\pi G_N} = \frac{Q}{\epsilon} = \frac{\alpha_S N}{\mathcal{J}}$, $m + \alpha$ is the mass of the black hole before the matter A goes out, and $t_R = (2m)^{-1} \ln(4mC)$. The exponential time shift slows down when $1 \sim 4\alpha C e^{\lambda_L(t_2 - t_1 - t_R)}$, namely at the scrambling time

$$t_* \sim \frac{1}{\lambda_L} \ln \frac{m}{\alpha} \sim \frac{1}{\lambda_L} \ln \frac{N}{q}, \quad (\text{D2})$$

where we find the correspondence of α in the SYK model by matching the energies of PETS on both sides, *i.e.* $4Cm\alpha = \langle \psi_\beta^1 | H | \psi_\beta^1 \rangle - \langle \mathbb{1}_\beta | H | \mathbb{1}_\beta \rangle = 2\mathcal{J}/q$. The $\ln(N/q)$ dependence in the scrambling time read from the OTOC agrees with the result of the complexities.

-
- [1] A Kitaev, A simple model of quantum holography (2015).
 - [2] Juan Maldacena and Douglas Stanford, “Remarks on the Sachdev-Ye-Kitaev model,” Phys. Rev. D **94**, 106002 (2016), arXiv:1604.07818 [hep-th].
 - [3] Yasuhiro Sekino and Leonard Susskind, “Fast Scramblers,” JHEP **10**, 065 (2008), arXiv:0808.2096 [hep-th].
 - [4] Patrick Hayden and John Preskill, “Black holes as mirrors: Quantum information in random subsystems,” JHEP **09**, 120 (2007), arXiv:0708.4025 [hep-th].
 - [5] Pavan Hosur, Xiao-Liang Qi, Daniel A. Roberts, and Beni Yoshida, “Chaos in quantum channels,” JHEP **02**, 004 (2016), arXiv:1511.04021 [hep-th].
 - [6] Daniel A. Roberts and Beni Yoshida, “Chaos and complexity by design,” JHEP **04**, 121 (2017), arXiv:1610.04903 [quant-ph].
 - [7] Daniel A. Roberts, Douglas Stanford, and Alexandre Streicher, “Operator growth in the SYK model,” JHEP **06**, 122 (2018), arXiv:1802.02633 [hep-th].

- [8] Xiao-Liang Qi and Alexandre Streicher, “Quantum Epidemiology: Operator Growth, Thermal Effects, and SYK,” *JHEP* **08**, 012 (2019), arXiv:1810.11958 [hep-th].
- [9] Adam Nahum, Sagar Vijay, and Jeongwan Haah, “Operator Spreading in Random Unitary Circuits,” *Phys. Rev. X* **8**, 021014 (2018), arXiv:1705.08975 [cond-mat.str-el].
- [10] Curt von Keyserlingk, Tibor Rakovszky, Frank Pollmann, and Shivaji Sondhi, “Operator hydrodynamics, OTOCs, and entanglement growth in systems without conservation laws,” *Phys. Rev. X* **8**, 021013 (2018), arXiv:1705.08910 [cond-mat.str-el].
- [11] Akash Goel, Ho Tat Lam, Gustavo J. Turiaci, and Herman Verlinde, “Expanding the Black Hole Interior: Partially Entangled Thermal States in SYK,” *JHEP* **02**, 156 (2019), arXiv:1807.03916 [hep-th].
- [12] Yuri D. Lensky, Xiao-Liang Qi, and Pengfei Zhang, “Size of bulk fermions in the SYK model,” (2020), arXiv:2002.01961 [hep-th].
- [13] Juan Martin Maldacena, “Eternal black holes in anti-de Sitter,” *JHEP* **04**, 021 (2003), arXiv:hep-th/0106112.
- [14] Leonard Susskind, “Why do Things Fall?” (2018), arXiv:1802.01198 [hep-th].
- [15] Adam R. Brown, Hrant Gharibyan, Alexandre Streicher, Leonard Susskind, Larus Thorlacius, and Ying Zhao, “Falling Toward Charged Black Holes,” *Phys. Rev. D* **98**, 126016 (2018), arXiv:1804.04156 [hep-th].
- [16] Henry W. Lin, Juan Maldacena, and Ying Zhao, “Symmetries Near the Horizon,” *JHEP* **08**, 049 (2019), arXiv:1904.12820 [hep-th].
- [17] Leonard Susskind, “Complexity and Newton’s Laws,” (2019), arXiv:1904.12819 [hep-th].
- [18] Leonard Susskind and Ying Zhao, “Complexity and Momentum,” (2020), arXiv:2006.03019 [hep-th].
- [19] Juan Maldacena, Douglas Stanford, and Zhenbin Yang, “Conformal symmetry and its breaking in two dimensional Nearly Anti-de-Sitter space,” *PTEP* **2016**, 12C104 (2016), arXiv:1606.01857 [hep-th].
- [20] Julius Engelsy, Thomas G. Mertens, and Herman Verlinde, “An investigation of AdS₂ backreaction and holography,” *JHEP* **07**, 139 (2016), arXiv:1606.03438 [hep-th].
- [21] Douglas Stanford and Leonard Susskind, “Complexity and Shock Wave Geometries,” *Phys. Rev. D* **90**, 126007 (2014), arXiv:1406.2678 [hep-th].
- [22] Adam R. Brown and Leonard Susskind, “Second law of quantum complexity,” *Phys. Rev. D* **97**, 086015 (2018), arXiv:1701.01107 [hep-th].
- [23] William Cottrell and Miguel Montero, “Complexity is simple!” *JHEP* **02**, 039 (2018), arXiv:1710.01175 [hep-th].
- [24] Run-Qiu Yang, Chao Niu, Cheng-Yong Zhang, and Keun-Young Kim, “Comparison of holographic and field theoretic complexities for time dependent thermofield double states,” *JHEP* **02**, 082 (2018), arXiv:1710.00600 [hep-th].
- [25] Run-Qiu Yang and Keun-Young Kim, “Time evolution of the complexity in chaotic systems: a concrete example,” *JHEP* **05**, 045 (2020), arXiv:1906.02052 [hep-th].
- [26] Ro Jefferson and Robert C. Myers, “Circuit complexity in quantum field theory,” *JHEP* **10**, 107 (2017), arXiv:1707.08570 [hep-th].
- [27] Run-Qiu Yang, Yu-Sen An, Chao Niu, Cheng-Yong Zhang, and Keun-Young Kim, “Principles and symmetries of complexity in quantum field theory,” *Eur. Phys. J. C* **79**, 109 (2019), arXiv:1803.01797 [hep-th].
- [28] Daniel E. Parker, Xiangyu Cao, Alexander Avdoshkin, Thomas Scaffidi, and Ehud Altman, “A Universal Operator Growth Hypothesis,” *Phys. Rev. X* **9**, 041017 (2019), arXiv:1812.08657 [cond-mat.stat-mech].
- [29] J.L.F. Barbn, E. Rabinovici, R. Shir, and R. Sinha, “On The Evolution Of Operator Complexity Beyond Scrambling,” *JHEP* **10**, 264 (2019), arXiv:1907.05393 [hep-th].
- [30] The Krylov basis generated by the Liouvillian can be incomplete in the Hilbert space $\mathcal{H} \otimes \mathcal{H}$.
- [31] J. M. Deutsch, “Quantum statistical mechanics in a closed system,” *Phys. Rev. A* **43**, 2046–2049 (1991).
- [32] Mark Srednicki, “Chaos and quantum thermalization,” *Phys. Rev. E* **50**, 888–901 (1994).
- [33] Marcos Rigol, Vanja Dunjko, and Maxim Olshanii, “Thermalization and its mechanism for generic isolated quantum systems,” *Nature* **452**, 854–858 (2008).
- [34] Leonard Susskind, “Computational Complexity and Black Hole Horizons,” *Fortsch. Phys.* **64**, 24–43 (2016), [Addendum: *Fortsch.Phys.* 64, 44–48 (2016)], arXiv:1403.5695 [hep-th].
- [35] Adam R. Brown, Daniel A. Roberts, Leonard Susskind, Brian Swingle, and Ying Zhao, “Complexity,

- action, and black holes,” *Phys. Rev. D* **93**, 086006 (2016), arXiv:1512.04993 [hep-th].
- [36] Adam R. Brown, Daniel A. Roberts, Leonard Susskind, Brian Swingle, and Ying Zhao, “Holographic Complexity Equals Bulk Action?” *Phys. Rev. Lett.* **116**, 191301 (2016), arXiv:1509.07876 [hep-th].
- [37] Zicao Fu, Alexander Maloney, Donald Marolf, Henry Maxfield, and Zhencheng Wang, “Holographic complexity is nonlocal,” *JHEP* **02**, 072 (2018), arXiv:1801.01137 [hep-th].
- [38] Run-Qiu Yang, “Complexity for quantum field theory states and applications to thermofield double states,” *Phys. Rev. D* **97**, 066004 (2018), arXiv:1709.00921 [hep-th].
- [39] Run-Qiu Yang, Yu-Sen An, Chao Niu, Cheng-Yong Zhang, and Keun-Young Kim, “To be unitary-invariant or not?: a simple but non-trivial proposal for the complexity between states in quantum mechanics/field theory,” (2019), arXiv:1906.02063 [hep-th].
- [40] Dean Carmi, Robert C. Myers, and Pratik Rath, “Comments on Holographic Complexity,” *JHEP* **03**, 118 (2017), arXiv:1612.00433 [hep-th].
- [41] Adam R. Brown, Hrant Gharibyan, Henry W. Lin, Leonard Susskind, Lrus Thorlacius, and Ying Zhao, “Complexity of Jackiw-Teitelboim gravity,” *Phys. Rev. D* **99**, 046016 (2019), arXiv:1810.08741 [hep-th].
- [42] Dean Carmi, Shira Chapman, Hugo Marrochio, Robert C. Myers, and Sotaro Sugishita, “On the Time Dependence of Holographic Complexity,” *JHEP* **11**, 188 (2017), arXiv:1709.10184 [hep-th].
- [43] Rong-Gen Cai, Misao Sasaki, and Shao-Jiang Wang, “Action growth of charged black holes with a single horizon,” *Phys. Rev. D* **95**, 124002 (2017), arXiv:1702.06766 [gr-qc].
- [44] Rong-Gen Cai, Shan-Ming Ruan, Shao-Jiang Wang, Run-Qiu Yang, and Rong-Hui Peng, “Action growth for AdS black holes,” *JHEP* **09**, 161 (2016), arXiv:1606.08307 [gr-qc].
- [45] Yu-Sen An, Rong-Gen Cai, and Yuxuan Peng, “Time Dependence of Holographic Complexity in Gauss-Bonnet Gravity,” *Phys. Rev. D* **98**, 106013 (2018), arXiv:1805.07775 [hep-th].
- [46] Rong-Gen Cai, Song He, Shao-Jiang Wang, and Yu-Xuan Zhang, “Revisit on holographic complexity in two-dimensional gravity,” (2020), arXiv:2001.11626 [hep-th].
- [47] Run-Qiu Yang, Hyun-Sik Jeong, Chao Niu, and Keun-Young Kim, “Complexity of Holographic Superconductors,” *JHEP* **04**, 146 (2019), arXiv:1902.07586 [hep-th].
- [48] Run-Qiu Yang, “Upper bound about cross-sections inside black holes and complexity growth rate,” (2019), arXiv:1911.12561 [hep-th].
- [49] Juan Maldacena, Douglas Stanford, and Zhenbin Yang, “Diving into traversable wormholes,” *Fortsch. Phys.* **65**, 1700034 (2017), arXiv:1704.05333 [hep-th].
- [50] Leonard Susskind and Ying Zhao, “Switchbacks and the Bridge to Nowhere,” (2014), arXiv:1408.2823 [hep-th].
- [51] Jos L.F. Barbn, Javier Martn-Garca, and Martin Sasieta, “Momentum/Complexity Duality and the Black Hole Interior,” (2019), arXiv:1912.05996 [hep-th].
- [52] Ning Bao and Junyu Liu, “Quantum complexity and the virial theorem,” *JHEP* **08**, 144 (2018), arXiv:1804.03242 [hep-th].
- [53] Adam R. Brown, Hrant Gharibyan, Geoff Penington, and Leonard Susskind, “The Python’s Lunch: geometric obstructions to decoding Hawking radiation,” (2019), arXiv:1912.00228 [hep-th].
- [54] Thomas G. Mertens, Gustavo J. Turiaci, and Herman L. Verlinde, “Solving the Schwarzian via the Conformal Bootstrap,” *JHEP* **08**, 136 (2017), arXiv:1705.08408 [hep-th].
- [55] Vijay Balasubramanian, Arjun Kar, Onkar Parrikar, Gbor Srosi, and Tomonori Ugajin, “Geometric secret sharing in a model of Hawking radiation,” (2020), arXiv:2003.05448 [hep-th].
- [56] Geoff Penington, Stephen H. Shenker, Douglas Stanford, and Zhenbin Yang, “Replica wormholes and the black hole interior,” (2019), arXiv:1911.11977 [hep-th].